ACS Catalysis

Article

Chameleon-Like Behavior of the Directing Group in the Rh(III)-Catalyzed Regioselective C-H Amidation of Indole: An Experimental and Computational Study

Jinquan Zhang, Hujun Xie, Hua-jian Zhu, Shuaizhong Zhang, Madhava Reddy Lonka, and Hong-Bin Zou

ACS Catal., **Just Accepted Manuscript** • DOI: 10.1021/acscatal.9b02512 • Publication Date (Web): 01 Oct 2019

is published by the American Chemical Society. 1155 Sixteenth Street N.W., Washington, DC 20036

Chameleon-Like Behavior of the Directing Group in the Rh(III)-Catalyzed Regioselective C−H Amidation of Indole: An Experimental and Computational Study

Jinquan Zhang,[†,⊥] *Hujun Xie,*[§,⊥] *Huajian Zhu,*[†‡,⊥] *Shuaizhong Zhang,*[†] *Madhava Reddy Lonka*[†] *and Hongbin Zou*[*,†]

[†] College of Pharmaceutical Sciences, Zhejiang University, Hangzhou, 310058, P. R. China

[§] Department of Applied Chemistry, Zhejiang Gongshang University, Hangzhou 310018, P. R. China

[‡] Zhejiang University City College, Hangzhou, 310015, P. R. China

ABSTRACT: The Rh(III)-catalyzed regioselective C−H amidation of *N*-methoxy-1*H*-indole-1-carboxamides by 1,4,2-dioxazol-5-ones was studied. *N*-methoxy amide, the directing group (DG) of interest, undergoes four different transformations through DG-retained, -coupled, -eliminated, or -migrated processes under moderately varied reaction conditions. Solvents, additives and temperature play important roles in these selective transformations: A trace addition of water

favors the functional group (FG)-assisted DG elimination; Extra addition of $K_2S_2O_8$ greatly enhances the formation of DG-coupled product; High temperature and proper FG together can shift the position of DG through intermolecular Friedel-Crafts-like acylation. The catalytic mechanisms underlying these reactions were further investigated through DFT calculations and experimental studies including the characterization of amido-inserted rhodacycle. An overall catalytic pathway was proposed to illustrate the reactions involved in the regioselective amidation of *N*-methoxy-1*H*-indole-1-carboxamide.

KEYWORDS: C−H activation, directing group, regioselective amidation, Friedel-Crafts-like acylation, DFT

INTRODUCTION

In the past few decades, transition-metal-catalyzed C−H bond activation, often incorporated in the organic manipulation of *N*-heterocyles,[1] has attracted wide attention from organic chemists, for being a highly efficient, atom-economical and environmentally benign synthetic tool.[2] Among the many forms of this methodology, directed C−H functionalization, first discovered in 1963, has recently reemerged as a reliable approach for achieving a diverse collection of carbon–carbon (C−C) and carbon–heteroatom (C−X) functionalization reactions.[3] This strategy introduces a directing group (DG) into a hydrocarbon substrate, and activates C−H bond through organometallic intermediates which ultimately convert the C−H bond to a functional group (FG). Various novel coordinating DGs have been designed and successfully installed onto the substrates of interest, where they promote the subsequent one-pot catalytic selective C−H functionalization through one of the three main pathways (Scheme 1a): (i) the majority of

installed DGs remain intact at the incorporated position;[4] (ii) some DGs further react with the inserted FG to form a cyclized product immediately following C−H activation;[5] and (iii) the rest DGs are readily eliminated *in situ* to produce desired products, which usually requires multiple chemical transformations and is not always achievable.[6] Taken together, these schemes infer unlimited synthetic capacity of DGs in catalytic site-selective preparation of structurally diversified products.

However, identifying DG and FG that are compatible with a target substrate is always challenging, as is determining the reaction conditions to robustly control the regioselectivity of C−H functionalization. In 2008, Yu's team reported the highly selective construction of C−C and C−N bonds through the directed activation of C−H bond using *N*-methoxy amides.[7] *N*-methoxy amide is a carbonyl-related DG consisting of a chelating amide and a methoxy group as nitrogen-protecting motif used in regioselective C−H functionalization.[8] This agent is particularly useful as a synthon, since *N*-methoxy amide can be readily converted to a number of synthetically versatile groups, including esters, amides and alkanes. Over the past ten years, *N*-methoxy amide has shown increasingly high success in forming C−C and C−X bonds *via* processes catalyzed by various transition-metals, such as rhodium, copper, palladium and ruthenium.[9–11] Different products with attractive structural features have been achieved through highly efficient one-pot regioselective reactions. In most cases, *N*-methoxy amide either remains on the products[9] or is further coupled with an adjacent FG to afford extra heterocycle.[10] A partial cleavage of the methoxy protecting group was also observed in some experiments.[11] However, complete detachment of *N*-methoxy amide from substrate following C−H functionalization has not yet been reported.

Inspired by the feasibility of using *N*-methoxy amide as an intramolecular DG, we investigated the directed regioselective amidation of *N*-methoxy amide-substituted indole **1** by the amidating reagent 1,4,2-dioxazol-5-one **2**[12] (Scheme 1b). This model study showed the versatile transformations of *N*-methoxy amide group under varied reaction conditions, including temperature, solvent and additive, whereby structurally attractive and diverse functionalized indoles **3**, **4**, **5** and **6** were achieved through Rh(III)-catalyzed C−H bond activation. In addition to incorporating FG at C2 to yield **3**, *N*-methoxy amide DG also acted as a coupling partner to give product **4** in tetrahydrofuran (THF) solvent at low temperature. Notably, the presence of a small amount of water led to the formation of DG-free product **5**, which demonstrates the first example of *in situ* elimination of *N*-methoxy amide. Moreover, product **6** was obtained after DG was shifted from N1 to C3 at high reaction temperature. Further experimental and computational studies were carried out to elucidate the underlying reaction mechanisms and reveal the cause of product diversity.

Scheme 1. Versatile DG Behavior in Transition-Metal Catalyzed C-H Bond Activation

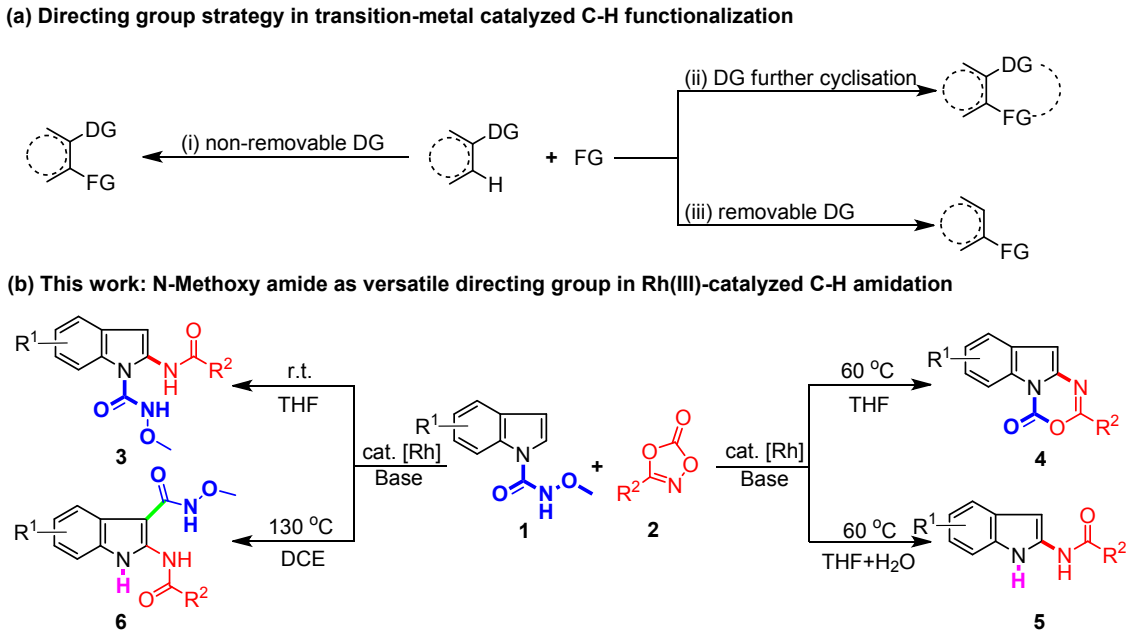

RESULTS AND DISCUSSION

Reaction Conditions Optimization. *N*-methoxy-1*H*-indole-1-carboxamide (**1a**) and 1,4,2-dioxazol-5-one (**2a**) were selected as starting materials to model the metal-mediated indole amidation. We began our optimization study by screening a wide range of reaction parameters, including catalysts, ligands, salt additives, solvents and temperatures (see Table S1–S4 in Supporting Information for detailed reaction condition screening). The simple mixture of commercially available complexes $[Cp^*RhCl_2]_2$ and $Zn(OTf)_2$ was used as the catalytic system, and solvent 1,2-dichloroethane (DCE) was applied initially. The reaction at room temperature formed a new C−N bond to give products **3a**, **4a**, **5a** and **6a**, in the yields of 52%, 9%, 17% and 7%, respectively (Table 1, entry 1). Replacing DCE with untreated THF (≤ 0.05% water) slightly improved the yield of **3a** and **5a** (Table 1, entry 2). And substituting CsOAc with NaOAc elevated the yield of **3a** to 88% (Table 1, entry 3), presumably due to the alkalinity difference between the two bases. Notably, raising the reaction temperature to 60 °C drastically decreased the yield of **3a** to less than 5% whereas the turnover of product **5a** was dramatically increased, and the yield of **4a** was also slightly improved (Table 1, entry 4). We next attempted the chemo-selective study of **4a** and **5a**. As shown in Table 1 (entries 5–7), a more balanced mixture of products **4a** and **5a** was obtained when anhydrous THF was employed as solvent, and replacing additive CsOAc with NaOAc/$K_2S_2O_8$ boosted the yield of **4a** from 24% to 78%, suggesting $K_2S_2O_8$ could promote the cyclization reaction. Since $KHSO_4$ has also been reported to assist similar cyclizations,[13] we attempted the reaction once more using NaOAc/$KHSO_4$ as the additive, and found the yield of **4a** was further increased to 81% (entry 8). Also of note, using untreated THF as solvent yielded slightly more **5a** than using anhydrous THF (Table 1, entries 4 and 5), indicating that the presence of water favors the production of **5a**. This result prompted us to add

10% water (v/v) into THF and as expected, the new solvent mixture gave distinct product **5a** in an excellent yield of 85% (Table 1, entry 9). However, same additional water into THF in entry 3 (Table 1) resulted in the slightly decreased yield of **3a** (Table S1, entry 10). To further explore the effect of temperature, we steadily raised it while keeping the rest conditions intact. Interestingly, the yield of product **6a** continuously increased until reaching 62% at 130 °C, whereas **3a**, **4a** and **5a** gradually diminished (Table 1, entries 10–12). The experimental outcomes also showed that the presence of CsOAc or NaOAc as an additive is crucial for the success of these transformations wherein $Cp^*Rh(OAc)_2$, rather than $[Cp^*RhCl_2]_2$, most likely acts as the active catalyst, as evidenced by the density functional theory (DFT) calculations (Figure S9, S10). Meanwhile, $Zn(OTf)_2$ was found to slightly increase the yield of **3a**, **5a** and **6a** (Table S1, S3 and S4) which might be ascribed to its promotion of the transformation $[Cp^*RhCl_2]_2$ to $Cp^*Rh(OAc)_2$ in the presence of CsOAc or NaOAc. We also screened the efficiency of various complexes containing the basic amide moiety (see Supporting Information for details). The results showed that *N*-methoxy amide outcompeted the rest of candidates in directing Rh(III)-catalyzed C−H amidation and promoting the subsequent transformations.

Table 1. Optimization of Reaction Conditions

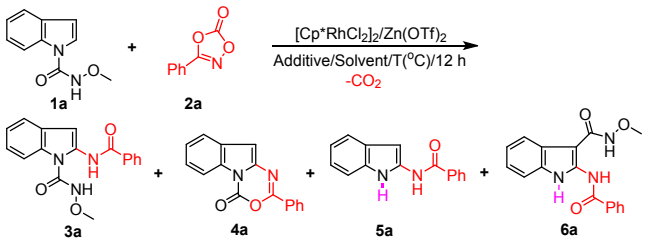

entry	solvent	additive	T (°C)	yield (%)[a]			
				3a	**4a**	**5a**	**6a**
1	DCE	CsOAc	r.t.	52	9	17	7
2	untreated THF	CsOAc	r.t.	68	<5	21	<5
3	**untreated THF**	**NaOAc**	**r.t.**	**88**	**<5**	**<5**	**<5**
4	untreated THF	CsOAc	60	<5	10	75	<5
5	anhydrous THF	CsOAc	60	<5	24	49	<5
6	anhydrous THF	NaOAc	60	<5	34	44	<5
7[b]	anhydrous THF	NaOAc $K_2S_2O_8$	60	<5	78	<5	<5
8[b]	**anhydrous THF**	**NaOAc $KHSO_4$**	**60**	<5	**81**	<5	<5
9	**THF/H_2O (10:1)**	**CsOAc**	**60**	<5	<5	**85**	<5
10	DCE	CsOAc	60	<5	12	51	24
11	DCE	CsOAc	95	<5	<5	25	48
12	**DCE**	**CsOAc**	**130**	<5	<5	<5	**62**

The reaction was conducted with **1a** (0.2 mmol), **2a** (0.24 mmol), $[Cp^*RhCl_2]_2$ (5 mol%), $Zn(OTf)_2$ (30 mol%), additive (0.2 mmol), solvent (2 mL), yield of isolated products.[a] Isolated yield; [b] $Zn(OTf)_2$ was not used.

Substrate Scope. With the optimized reaction conditions in hand, we sought to evaluate the substrate scope of these processes, starting with the formation of DG-retained product **3** using the same catalytic system as shown in Table 1 (entry 3). The results showed that the mono-substituted 3-phenyl dioxazolones were well tolerated in the reaction with **1a**, affording **3a**–**3g**, **3j** and **3k** in good to excellent isolated yields ranging from 72% to 92% (Scheme 2). The dioxazolones containing electron-withdrawing group at *para*-position of the phenyl ring, such as

fluorine, chlorine and trifluoromethyl group, gave higher yield of products (**3d**, **3e** and **3g**) than those with electron-donating group. This trend was further verified by the high yield of **3m** (83%) derived from dioxazolones containing 3, 4-chloro group on the phenyl ring. However, *para*-methyl ester or cyano substituents on phenyl ring prevented dioxazolones from producing desired product (**3h** and **3i**). Meanwhile, more sterically hindered diphenyl-substituted dioxazolone resulted in much lower yield (**3l**, 56%). In addition, we found alkyl-substituted dioxazolone also compatible to react with **1a** to afford **3n** in moderate yield. Similarly tolerated was the dioxazolone bearing styryl substituent as a conjugated side chain (**3o**). Moreover, dioxazolones with thiophene substituent reacted with **1a** smoothly, giving **3p** in good yield. Subsequently, we investigated the scope of *N*-methoxy amide-substituted indoles. As a result, a variety of electron-donating and -withdrawing substituents on phenyl ring of indole were well tolerated in the reaction, affording the corresponding desired products (**3q**–**3t** and **3x**–**3ab**) in moderate to good yields ranging from 57% to 86%, with the exception of the compounds with strong electrophilic methyl ester, nitro or cyano substituents (**3u**–**3w**).

Scheme 2. Synthesis of Products 3 with DG Retained

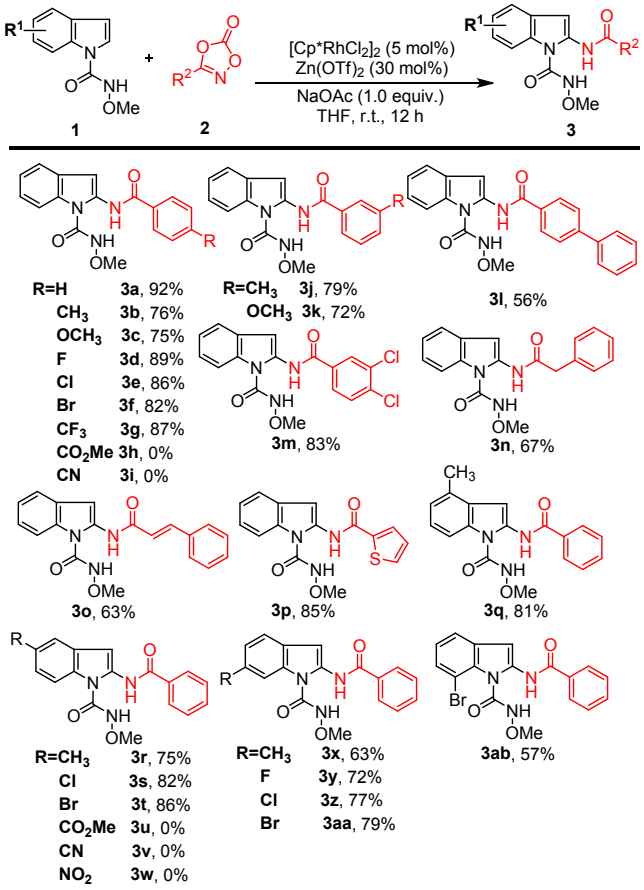

The reaction was conducted with **1** (0.2 mmol), **2** (0.24 mmol), $[Cp^*RhCl_2]_2$ (5 mol%), $Zn(OTf)_2$ (30 mol%), NaOAc (0.2 mmol), THF (2 mL), room temperature, yield of isolated products.

Next, we surveyed the substrate scope for the synthesis of DG-coupled products, 4*H*-[1,3,5]oxadiazino[3,4-a]indol-4-ones (**4**, Scheme 3). A broad range of indoles and aryl-dioxazolones were investigated for their reaction compatibility. Dioxazolones, whether bearing neutral hydrogen or phenyl, electron-donating methyl or methoxy, or electron-withdrawing fluoro or chloro on the phenyl ring, all successfully reacted with **1a** to give corresponding products in moderate to good isolated yields (**4a**–**4h**), among which **4d**, derived from phenyl-substituted phenyl-dioxazolone, was achieved in the highest yield of 91%. Employing naphthalene, benzyl or styryl-substituted dioxazolones as substrates resulted in moderate yields

of the desired products (**4i**–**4k**). Similar yields were obtained by replacing the substituents of dioxazolone with heterocycles, such as furan and thiophene (**4l** and **4m**). Indoles bearing different groups were also found compatible in the coupling assembly of the corresponding cyclized heterocycles (**4n**–**4z**), albeit in slightly lower yields.

Scheme 3. Synthesis of Product 4 with DG Coupled

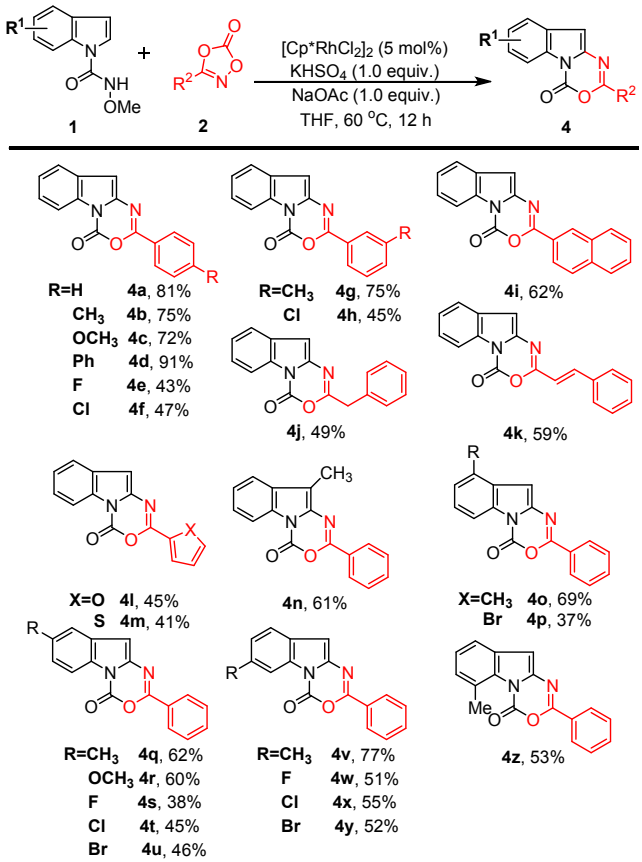

The reaction was conducted with **1** (0.2 mmol), **2** (0.24 mmol), $[Cp^*RhCl_2]_2$ (5 mol%), NaOAc (0.2 mmol), $KHSO_4$ (0.2 mmol), THF (2 mL), 60 °C, yield of isolated products.

Notably, a unique reaction occurred when we replaced DCE with aqueous THF as the reaction solvent: An elimination of the DG took place *in situ* following the successful insertion of the substituted amide unit to C2 position of the indole ring of **1**, leading to the formation of DG-free product **5** (Scheme 4). The substrate scope and reaction limitatio.ns were accordingly examined.

The results indicated that the electron-donating substituents on the phenyl ring of dioxazolones resulted in higher isolated yields of products (**5b**, **5c** and **5g**) than those obtained with electron-withdrawing substituents (**5d**–**5f** and **5h**). When using naphthalene, benzyl and styryl-substituted dioxazolone as substrates, the desired products were yielded in moderate to good amount (**5i**–**5k**). We then extended the phenyl substituents of dioxazolones to alkyls and heterocycles, and found that isobutyl and furan-dioxazolone were also viable in forming desired products (**5l** and **5m)**, albeit in slightly lower yields. In addition, substrates with *N*-carboxamides substituted on various positions of indole ring efficiently generated *N*-(indol-2-yl)amides in moderate to good yields (**5n**–**5x**).

Scheme 4. Synthesis of Product 5 with DG Eliminated

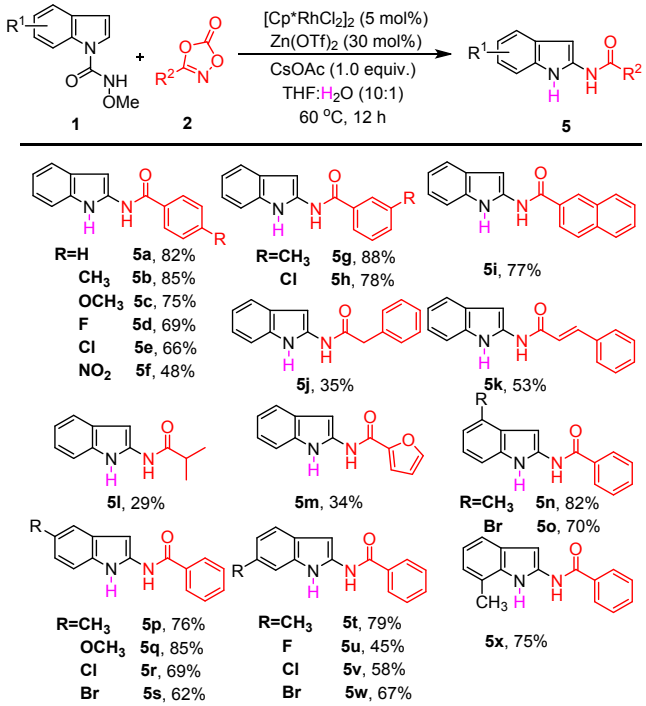

The reaction was conducted with **1** (0.2 mmol), **2** (0.24 mmol), $[Cp^*RhCl_2]_2$ (5 mol%), $Zn(OTf)_2$ (30 mol%), CsOAc (0.2 mmol), THF (2 mL), H_2O (0.2 mL), 60 °C, yield of isolated products.

As shown in Scheme 5, *N*-methoxy-1*H*-indole-1-carboxamide (**1a**) reacted smoothly with various aromatic dioxazolones to introduce the FG to C2 position of the indole ring while transferring the DG from N-1 to C-3, which then generated desired products (**6a**−**6g**) in moderate to good isolated yields. Using **1a** derivatives bearing electron-donating methyl or methoxy groups on aromatic ring also afforded the desired products **6h** and **6i** in good yields. However, no observable target product was generated from **1a** or **2a** containing an electron-withdrawing substituent such as chloro or bromo group.

Scheme 5. Synthesis of Product 6 with DG Migrated

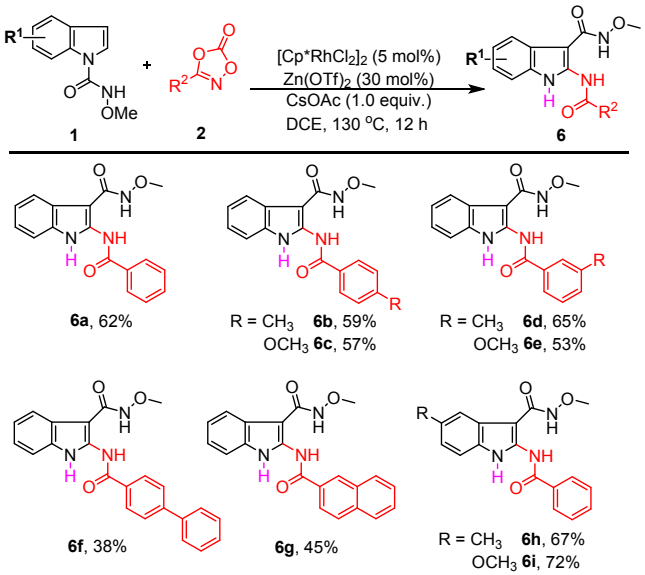

The reaction was conducted with **1** (0.2 mmol), **2** (0.24 mmol), $[Cp^*RhCl_2]_2$ (5 mol%), $Zn(OTf)_2$ (30 mol%), CsOAc (0.2 mmol), DCE (2 mL), 130 °C, yield of isolated products.

Mechanistic Studies. The versatile *N*-methoxy amide DG has exhibited great synthetic capacity by successfully furnishing four different series of indole amidation products through Rh(III)-catalyzed C−H activation. To gain insight into the pathways underlying the reaction and its diversity, we conducted mechanistic investigations using a combined experimental and computational methodology to address specifically: (1) What is the key intermediate in the

synthesis of products **3a**, **4a**, **5a** or **6a**? (2) What cascade steps it takes for these four transformations to take place? (3) Why does the C−H amidation prefer the site of C2 instead of C7 in similar proximity? (4) How do DG elimination and DG migration occur in the synthesis of **5** and **6**, respectively?

Scheme 6. Intermediate Study for the Amidation

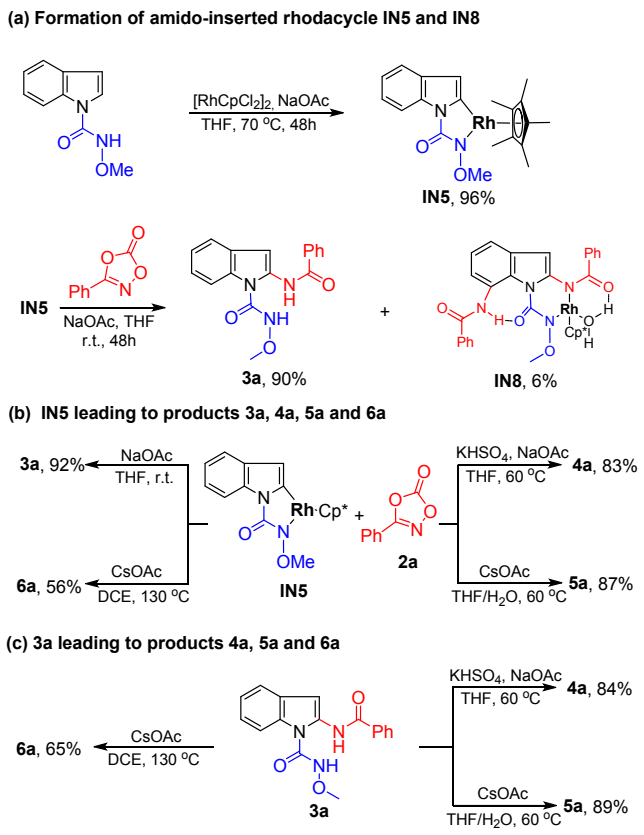

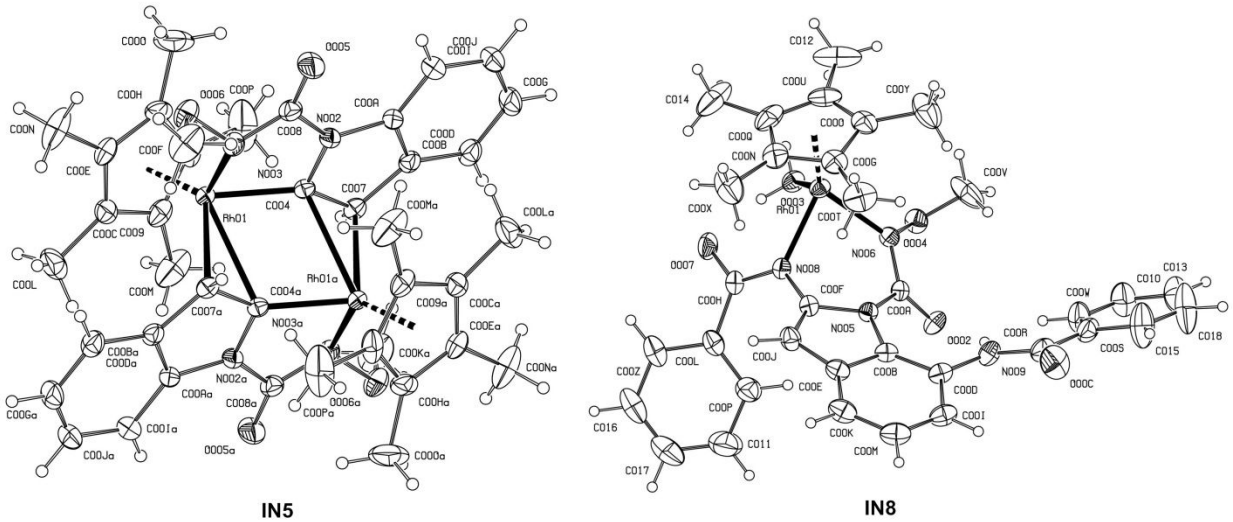

Figure 1. Molecular structure and atom numbering scheme for **IN5** and **IN8**.

In order to investigate all the possible intermediates, we first obtained a stable five-membered rhodacycle **IN5** by treating substrate **1a** with $[Cp^*RhCl_2]_2$ at 70 °C as shown in Scheme 6a. The subsequent reaction between **IN5** and **2a** successfully afforded product **3a** in excellent yield as well as a small amount of di-amidated Rh complex **IN8**. Both intermediates **IN5** and **IN8** were confirmed by X-ray crystallography (Figure 1). Next, we achieved products **3a**, **4a**, **5a** and **6a** in 92%, 83%, 87% and 56% yield respectively, by coupling **IN5** with **2a** under different conditions (entries 3, 7, 8 and 11, Table 1) without employing additional $[Cp^*RhCl_2]_2$ (Scheme 6b). This finding suggests that **IN5** very likely acts as an intermediate in C−H activation to afford desired products. In order to verify the role of **3a** in the formation of the rest products, we subjected it to the standard conditions without adding $[Cp^*RhCl_2]_2$. As a result, products **4a**, **5a** and **6a** were isolated in yields of 84%, 89% and 65% respectively (Scheme 6c), suggesting that **3a** is most likely the central intermediate to form the three other products.

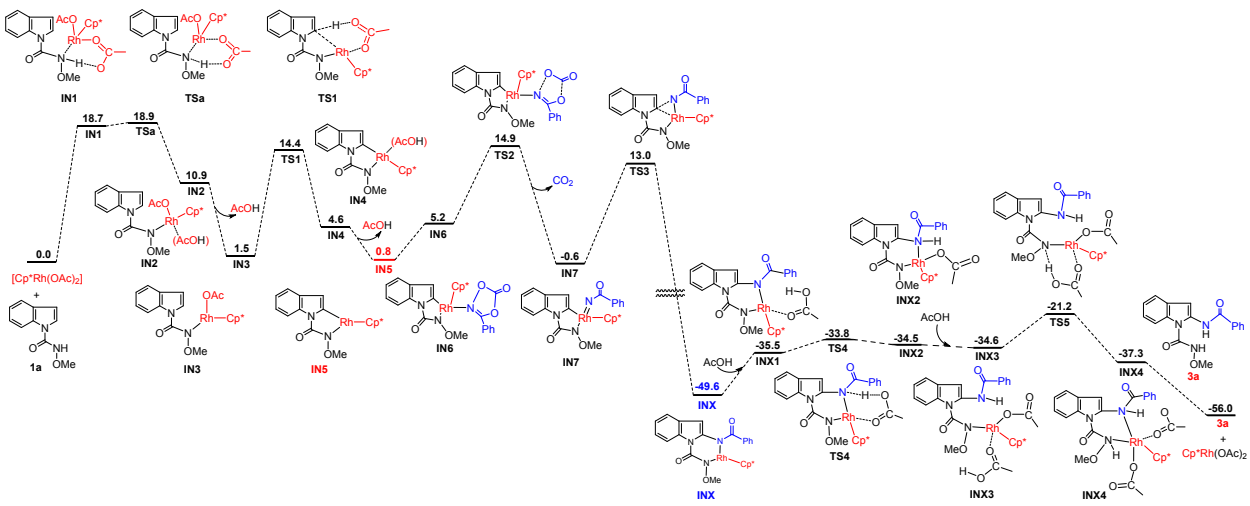

Figure 2. Free energy profiles (kcal mol^{-1}) for the generation of **3a** from **1a** and **2a**.

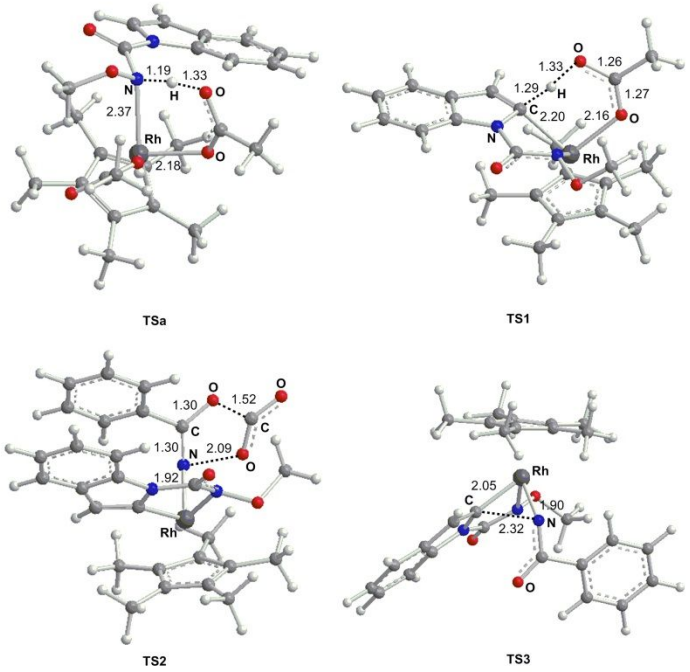

Figure 3. Optimized structures (Å) for selected transition states as shown in Figure 2.

In order to further study the mechanism to form **3a**, we conducted a series of density functional theory (DFT) calculations at the level of M06[14] using the Gaussian 09 suite of computational

programs[15]. (see Supporting Information for computational details). The Rh and Cl atoms were described by the Lanl2dz basis set and effective core potential.[16] The 6-31G(d,p) basis set[17] was applied for the C, H, O and N atoms. In addition, polarization functions of Rh(ζf) = 1.350 and Cl(ζd) = 0.514 were added.[18] Frequencies were calculated at the same level of theory to obtain the thermodynamic corrections and to confirm whether the structures were minima (no imaginary frequency) or transition states (only one imaginary frequency). Intrinsic reaction coordinate (IRC) calculations[19] were conducted to confirm all transition-state structures that connected the proposed reactants and products. The most plausible pathway from **1a** to **3a** was then identified among several proposed routes (see Supporting Information). As shown in Figure 2, starting material **1a** is initially coordinated to the catalyst to form a complex that undergoes subsequent deprotonation by OAc^- twice and transforms to the intermediate **IN5**, confirmed by X-ray crystallography. A kinetic isotope effect (KIE) study (k_H/k_D = 1.31, see Supporting Information) suggested that the C−H bond cleavage at the *ortho*-position of the indole is not the rate determining step, a finding consistent with the KIE result of **TS1** (k_H/k_D = 1.46) from the DFT calculation (Figure 2). Next, the other starting material **2a** is coordinated to Rh(III) complex **IN5** to give **IN6** with an endergonicity of 4.4 kcal/mol, which is followed by the CO_2 release through **TS2** (Figure 3) with a barrier of 16.6 kcal/mol. **IN7** further carries out a C−N bond coupling, which has a barrier of 13.6 kcal/mol, to transiently form **TS3** wherein the C-Rh(III) bond was cleaved to deliver intermediate **INX**. However, the six-membered rhodacycle **INX** was not detected throughout our experiment, presumably because **INX** is so reactive that it converts to **3a** immediately after formation. Subsequently, the coupling of **INX** to acetic acid leads to **TS4** *via* **INX1**and the following protonation of **TS4** gives rise to **INX2**. Further coordination of additional acetic acid to Rh(III) on **INX2** and the N-Rh(III) bond cleavage together generate **TS5**

via **INX3**, which ultimately results in the formation of the final product **3a** through **INX4** and the regeneration of catalyst Cp*Rh(OAc)$_2$.

Scheme 7. Selective C−H Activation of C2 Over C7

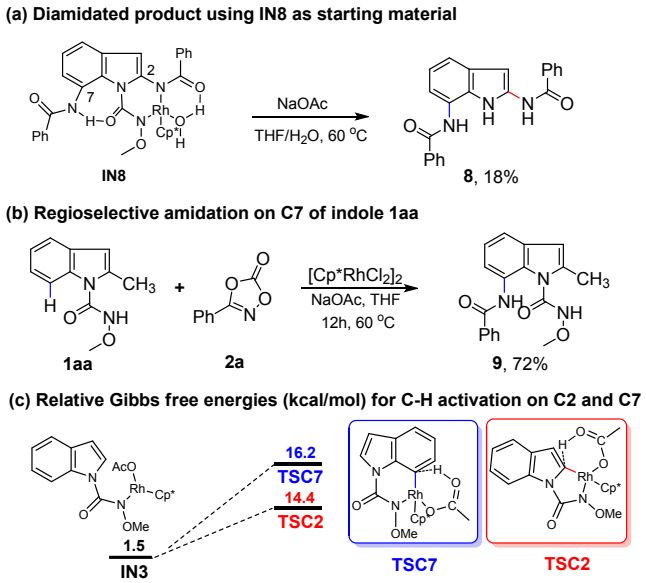

It is noteworthy that during the treatment of **IN5** with **2a** (Scheme 6a), a small amount of **IN8**, exhibiting C−H activation potential at C7, was alternatively obtained in place of **INX**. We thus continued investigation using this di-amidated intermediate as a starting material under various standard conditions excluding the addition of [Cp*RhCl$_2$]$_2$. As a result, none of the products **3a**, **4a**, **5a** or **6a** was detected. Instead, compound **8** with amidation on both C2 and C7 of indole was obtained (Scheme 7a). The C−H activation on C7 was further confirmed by reaction between C2-methylated **1aa** and **2a**, which led to product **9** in good yield (Scheme 7b). However, no C7-amidated product was observed in the reaction between **1a** and **2a**, suggesting that the C−H activation at C2 was favored in this catalytic system.

To understand the cause of this distinct selectivity, we computationally analyzed the relative Gibbs free energies of C−H activation for both sites C2 and C7. Scheme 7c shows that C2 exhibits relatively lower energy barrier (12.9 kcal/mol) than C7 (14.7 kcal/mol), hence being the preferred activating site. This finding accords with our experimental results shown in Scheme 2, 7a and 7b, and explains the regioselectivity observed with *N*-methoxy-1*H*-indole-1-carboxamide (**1a**).

Also of note, the carbonyl group on the cyclized product **4** has several possible sources: starting material **1** or **2**, or their spontaneous decomposition product CO_2. Through stable-isotope labeling experiments with ^{13}C, we were able to clarify that the carbonyl group comes straight from **1**, a finding that is consistent with Scheme 6c (see Supporting Information for more details).

To our surprise, product **5a** and **6a** were also formed through intermediate **3a**, indicating that DG elimination and translocation took place during the process (Scheme 6c). This very unusual observation prompted us to investigate the underlying mechanisms. As shown in Scheme 8a, compound **1a** did not afford DG-free indole under the same elimination condition of **3a** (Scheme 8a), suggesting that the amidation of **3a** contributes to the DG removal, presumably by increasing the electron density of the adjacent nitrogen to which DG was attached. This effect of FG on the translocation of DG was also detected in the transformation of **3a** under the standard condition to form **6a** (Scheme 8b), in contrast to the reaction of **1a** or **1aa** wherein no DG migration was observed. As shown in Scheme 8b, instead of giving any DG-shifted product, moderate electron-donating 2-methyl-substituted **1aa** delivered mainly DG-free product **10** in 45% isolated yield, along with remaining **1aa**. However, when **5a** reacted with **1aa** in a 1:1 ratio, the DG-shifted product **6a** was obtained in 53% isolated yield and compound **10** was produced in 75% yield, leaving no traceable unreacted **1aa**. Taken together, these outcomes indicate that the

migration of DG from N1 to C3 might also be attributed to the electron-donating effect of the amide FG in proximity which activates the amidation of C3 by enhancing its electronegativity and hence accelerating the translocation of DG.

Scheme 8. FG Effect on DG Elimination and Migration

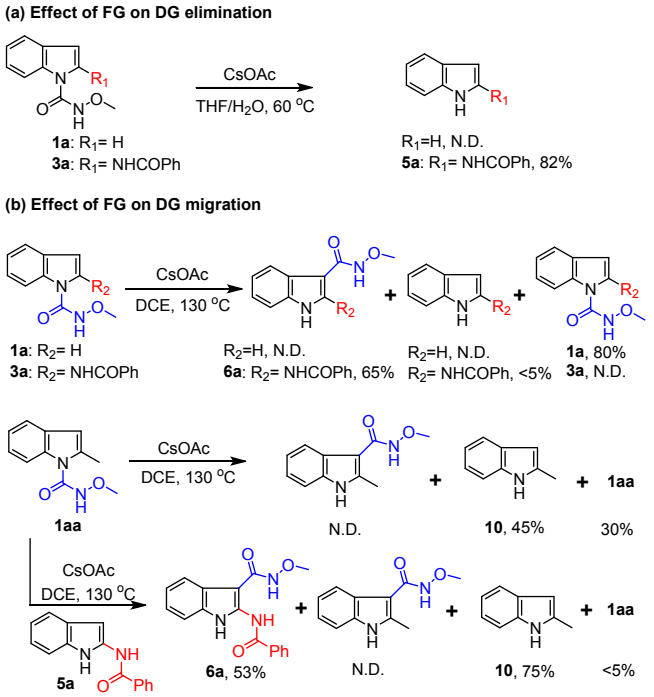

On the basis of the experimental and computational results, we propose four plausible mechanisms underlying the C-H bond functionalization as shown in Scheme 9. In the presence of CsOAc, dimeric compound $[Cp^*RhCl_2]_2$ transforms to $Cp^*Rh(OAc)_2$, which is then captured by **1a** to afford rhodacycle **IN5** through *N*-metalation and turnover-limiting C−H activation. The transmetalation of **IN5** by **2a** at room temperature leads to product **3a** as well as a small amount of **IN8**, which presumably gives the proposed intermediate **INX** during the reaction. The fact that no **INX** was detected could be ascribed to its high instability. Next, *ortho*-amidated product **3a** serves as a key intermediate to form **4a**, **5a** and **6a**. In the presence of NaOAc, the

tautomerization of **3a** takes place to give **A** which then undergoes lactonization to ultimately furnish DG-coupled product **4a** *via* [4+2] cyclization. On a parallel pathway, the DG of **3a** is removed by base CsOAc to obtain **B** followed by protonation in the presence of water, which eventually leads to the formation of DG-free product **5a**. Meanwhile, at high temperature, the electron rich C3 of the same intermediate **B** could also attack the carbonyl group in DG of **3a** through the intermolecular Friedel-Crafts-like acylation to form product **6a**, and regenerate molecule of **B** to continuously drive the reaction cycle.

Scheme 9. Proposed Reaction Pathways

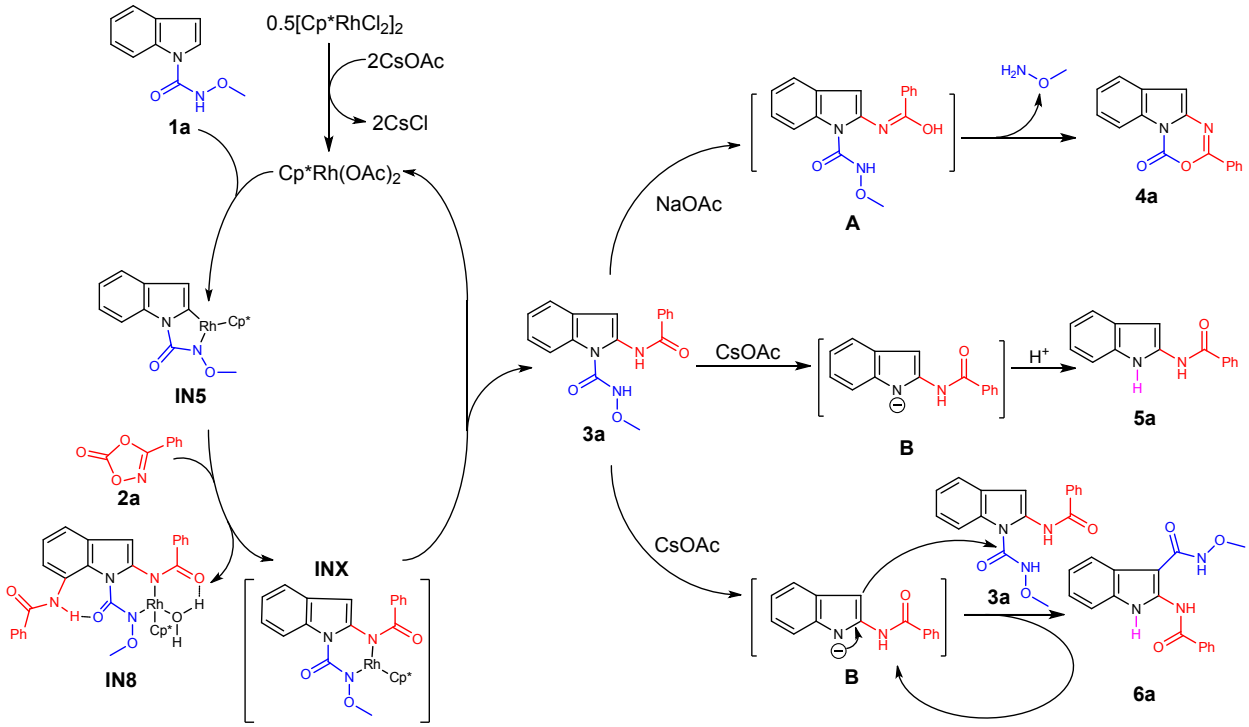

CONCLUSION

In summary, we developed rhodium-catalyzed regioselective C−H amidation of indoles and obtained four different products under moderately varied reaction conditions. The four ways of C-H functionalization were achieved by fully utilizing the reacting potential of *N*-methoxy amide

as intramolecular DG of *N*-methoxy-1*H*-indole-1-carboxamides when interacting with 1,4,2-dioxazol-5-ones. The traditional mechanism of C−H activation, assisted by *N*-methoxy amide DG, successfully introduces amide FG to the indole moiety to produce compound **3**. A slight modification of reaction conditions overrides the conventional mechanism and renders the chelating carbonyl group of DG so much more reactive that it forms a further coupled product **4**. Notably, the addition of a small amount of water results in an *in situ* elimination of DG to give product **5**, the first time *N*-methoxy amide acts as a completely removable DG. Furthermore, unprecedented DG migration gives rise to unexpected product **6**, a process accelerated by high reaction temperature and facilitated by *ortho*-amidated intermediate **3**. To our best knowledge, this is the first case of DG migration occurring in directed transition-metal-catalyzed C−H functionalization wherein the newly installed FG plays a crucial role in the intermolecular Friedel-Crafts-like acylation. Mechanistic studies involving both experimental and theoretical methodologies were carried out. Two Cp*Rh(III) complexes were isolated and characterized. The DFT calculations revealed the possible pathway to obtain **3a** and explained preferred C−H activation site of C2 over C7 on *N*-methoxy-1*H*-indole-1-carboxamide (**1a**). This rhodium-catalyzed reaction provides a facile approach to indole amidation with high regioselectivity, tolerates a broad range of substrates and efficiently produces a variety of indoles through one-pot DG-coupled, -eliminated or -migrated reactions. The enabling manipulations significantly expand the synthetic utility of *N*-methoxy amide, be it an easily accessible directing agent, a C-H functional building block, a removable group or a potentially transferable moiety. Such versatile strategy and its extension may encourage researchers to discover more promising DGs for transition-metal-catalyzed C−H bond activation, making available new targets and materials that would have been previously out of range.

ASSOCIATED CONTENT

Supporting Information

The Supporting Information is available free of charge on the ACS Publications website at DOI:

^{1}H and ^{13}C NMR spectra of all newly synthesized compounds (PDF)

AUTHOR INFORMATION

Corresponding Author

* zouhb@zju.edu.cn

ORCID

Hong-Bin Zou: 0000-0001-6784-2737

Author Contributions

⊥J.-Q.Z., H.-J.X., and H.-J.Z. contributed equally to this work.

Notes

The authors declare no competing financial interest.

ACKNOWLEDGMENT

This work was supported by the National Natural Science Foundation of China (No. 21472170), the Zhejiang Provincial Fund for Distinguished Young Scholars (LR15B020001). We thank Prof. Yongping Yu and Prof. Sunliang Cui (Zhejiang University, China) for useful discussions, Dr. Supakarn Chamni (Chulalongkorn University, Thailand) for thoughtful suggestion toward manuscript preparation.

REFERENCES

(1) (a) Kalepu, J.; Gandeepan, P.; Ackermann, L.; Pilarski, L. T., C4–H Indole Functionalisation: Precedent and Prospects. *Chem. Sci.* **2018,** *9*, 4203–4216. (b) Nagae, H.; Kundu, A.; Inoue, M.; Tsurugi, H.; Mashima, K., Functionalization of the C−H Bond of N–Heteroaromatics Assisted by Early Transition-Metal Complexes. *Asian J. Org. Chem.* **2018,** *7*, 1256–1269. (c) Das, R.; Kapur, M., Transition-Metal-Catalyzed C−H Functionalization Reactions of π-Deficient Heterocycles. *Asian J. Org. Chem.* **2018,** *7*, 1217–1235. (d) Vorobyeva, D. V.; Osipov, S. N., Selective Synthesis of 2-and 7-Substituted Indole Derivatives *via* Chelation-Assisted Metallocarbenoid C–H Bond Functionalization. *Synthesis* **2018,** *50*, 227–240. (e) Leitch, J. A.; Bhonoah, Y.; Frost, C. G., Beyond C2 and C3: Transition-Metal-Catalyzed C–H Functionalization of Indole. *ACS Catal.* **2017,** *7*, 5618–5627. (f) Aziz, J.; Piguel, S., An Update on Direct C–H Bond Functionalization of Nitrogen-Containing Fused Heterocycles. *Synthesis* **2017,** *49*, 4562–4585. (g) Sandtorv, A. H., Transition Metal-Catalyzed C–H Activation of Indoles. *Adv. Synth. Catal.* **2015,** *357*, 2403–2435.

(2) (a) Thompson, S. J.; Brennan, M. R.; Lee, S. Y.; Dong, G. Synthesis and applications of Rhodium Porphyrin Complexes. *Chem. Soc. Rev.* **2018**, *47*, 929−981. (b) Abrams, D. J.; Provencher, P. A.; Sorensen, E. J. Recent Applications of C–H Functionalization in Complex Natural Product Synthesis. *Chem. Soc. Rev.* **2018**, *47*, 8925–8967. (c) Ma, C.; Fang, P.; Mei, T.-S. Recent Advances in C–H Functionalization Using Electrochemical Transition Metal Catalysis. *ACS Catal.* **2018**, *8*, 7179–7189. (d) Karimov, R. R.; Hartwig, J. F. Transition-Metal-Catalyzed Selective Functionalization of C(sp^3)−H Bonds in Natural Products. *Angew. Chem. Int. Ed.* **2018**, *57*, 4234–4241. (e) Kim, D.-S.; Park, W.-J.; Jun, C.-H. Metal–Organic Cooperative Catalysis in C–H and C–C Bond Activation. *Chem. Rev.* **2017**, *117*, 8977–9015. (f) Park, Y.; Kim, Y.;

Chang, S. Transition Metal-Catalyzed C–H Amination: Scope, Mechanism, and Applications. *Chem. Rev.* **2017**, *117*, 9247–9301. (g) Qi, X.; Li, Y.; Bai, R.; Lan, Y. Mechanism of Rhodium-Catalyzed C–H Functionalization: Advances in Theoretical Investigation. *Acc. Chem. Res.* **2017**, *50*, 2799−2808. (h) Piou, T.; Rovis, T. Electronic and Steric Tuning of a Prototypical Piano Stool Complex: Rh (III) Catalysis for C–H Functionalization. *Acc. Chem. Res.* **2017**, *51*, 170−180. (i) Gensch, T.; Hopkinson, M.; Glorius, F.; Wencel-Delord, J. Mild Metal-Catalyzed C–H Activation: Examples and Concepts. *Chem. Soc. Rev.* **2016**, *45*, 2900–2936. (j) Park, Y.; Ahn, S.; Kang, D.; Baik, M.-H. Mechanism of Rh-Catalyzed Oxidative Cyclizations: Closed Versus Open Shell Pathways. *Acc. Chem. Res.* **2016**, *49*, 1263−1270. (k) Ye, B.; Cramer, N. Chiral Cyclopentadienyls: Enabling Ligands for Asymmetric Rh (III)-Catalyzed C–H Functionalizations. *Acc. Chem. Res.* **2015**, *48*, 1308–1318. (l) Sperger, T.; Sanhueza, I. A.; Kalvet, I.; Schoenebeck, F. Computational Studies of Synthetically Relevant Homogeneous Organometallic Catalysis Involving Ni, Pd, Ir, and Rh: an Overview of Commonly Employed DFT Methods and Mechanistic Insights. *Chem. Rev.* **2015**, *115*, 9532–9586. (m) DeAngelis, A.; Panish, R.; Fox, J. M. Rh-Catalyzed Intermolecular Reactions of α-Alkyl-α-diazo Carbonyl Compounds with Selectivity over β-Hydride Migration. *Acc. Chem. Res.* **2015**, *49*, 115–127. (n) Lewis, J. C.; Bergman, R. G.; Ellman, J. A. Direct Functionalization of Nitrogen Heterocycles via Rh-Catalyzed C−H Bond Activation. *Acc. Chem. Res.* **2008**, *41*, 1013–1025.

(3) (a) Sambiagio, C.; Schönbauer, D.; Blieck, R.; Dao-Huy, T.; Pototschnig, G.; Schaaf, P.; Wiesinger, T.; Zia, M. F.; Wencel-Delord, J.; Besset, T. A Comprehensive Overview of Directing Groups Applied in Metal-Catalysed C–H Functionalisation Chemistry. *Chem. Soc. Rev.* **2018**, *47*, 6603–6743. (b) Zhang, F. L.; Hong, K.; Li, T. J.; Park, H.; Yu, J. Q. Functionalization of C(sp^3)–H Bonds Using a Transient Directing Group. *Science* **2016**, *351*,

252–256. (c) Liu, Z. J.; Lu, X.; Wang, G.; Li, L.; Jiang, W. T.; Wang, Y. D.; Xiao, B.; Fu, Y. Directing Group in Decarboxylative Cross-coupling: Copper-Catalyzed Site-Selective C–N Bond Formation from Nonactivated Aliphatic Carboxylic Acids. *J. Am. Chem. Soc.* **2016**, *138*, 9714–9719. (d) Zhu, R. Y.; Farmer, M. E.; Chen, Y. Q.; Yu, J. Q. A Simple and Versatile Amide Directing Group for C−H Functionalizations. *Angew. Chem. Int. Ed.* **2016**, *55*, 10578–10599. (e) Piou, T.; Rovis, T. Rhodium-Catalysed *syn*-Carboamination of Alkenes via a Transient Directing Group. *Nature* **2015**, *527*, 86–90. (f) Murai, S.; Kakiuchi, F.; Sekine, S.; Tanaka, Y.; Kamatani, A.; Sonoda, M.; Chatani, N. Efficient Catalytic Addition of Aromatic Carbon-Hydrogen Bonds to Olefins. *Nature* **1993**, *366*, 529–531. (g) Kleiman, J. P.; Dubeck, M. The Preparation of Cyclopentadienyl [*o*-(phenylazo)phenyl] Nickel. *J. Am. Chem. Soc.* **1963**, *85*, 1544–1545.

(4) (a) Kapoor, M.; Chand-Thakuri, P.; Young, M. C., Carbon Dioxide-Mediated C(sp^2)–H Arylation of Primary and Secondary Benzylamines. *J. Am. Chem. Soc.* **2019**, *141*, 7980−7989; (b) Zhao, K.; Du, R.; Wang, B.; Liu, J.; Xia, C.; Yang, L., $RhCl_3 \cdot 3H_2O$-Catalyzed Regioselective C(sp^2)–H Alkoxycarbonylation: Efficient Synthesis of Indole- and Pyrrole-2-carboxylic Acid Esters. *ACS Catal.* **2019**, *9*, 5545–5551. (c) Yang, X.; Zheng, G.; Li, X. Rhodium(III)-Catalyzed Enantioselective Coupling of Indoles and 7-Azabenzonorbornadienes by C−H Activation/Desymmetrization. *Angew. Chem. Int. Ed.* **2019**, *131*, 328–332. (d) Li, M.; Kwong, F. Y., Cobalt-Catalyzed Tandem C−H Activation/C−C Cleavage/C−H Cyclization of Aromatic Amides with Alkylidenecyclopropanes. *Angew. Chem. Int. Ed.* **2018**, *57*, 6512–6516. (e) Piou, T.; Romanov-Michailidis, F.; Romanova-Michaelides, M.; Jackson, K. E.; Semakul, N.; Taggart, T. D.; Newell, B. S.; Rithner, C. D.; Paton, R. S.; Rovis, T. Correlating Reactivity and Selectivity to Cyclopentadienyl Ligand Properties in Rh(III)-Catalyzed C–H Activation Reactions: An Experimental and Computational Study. *J. Am. Chem. Soc.* **2017**, *139*, 1296–1310.

(f) Lied, F.; Lerchen, A.; Knecht, T.; Mück-Lichtenfeld, C.; Glorius, F. Versatile Cp*Rh(III)-Catalyzed Selective *Ortho*-Chlorination of Arenes and Heteroarenes. *ACS Catal.* **2016**, *6*, 7839–7843.

(5) (a) Hassan, I. S.; Ta, A. N.; Danneman, M. W.; Semakul, N.; Burns, M.; Basch, C. H.; Dippon, V. N.; McNaughton, B. R.; Rovis, T. Asymmetric *δ*-Lactam Synthesis with a Monomeric Streptavidin Artificial Metalloenzyme. *J. Am. Chem. Soc.* **2019**, *141*, 4815−4819. (b) Vidal, X.; Mascareñas, J. L.; Gulías, M., Palladium-Catalyzed, Enantioselective Formal Cycloaddition between Benzyltriflamides and Allenes: Straightforward Access to Enantioenriched Isoquinolines. *J. Am. Chem. Soc.* **2019**, *141*, 1862–1866. (c) Yin, J.; You, J. Concise Synthesis of Polysubstituted Carbohelicenes by a C−H Activation/Radical Reaction/C−H Activation Sequence. *Angew. Chem. Int. Ed.* **2019**, *58*, 302–306. (d) Escudero, J.; Bellosta, V.; Cossy, J. Rhodium-Catalyzed Cyclization of *O*,ω-Unsaturated Alkoxyamines: Formation of Oxygen-Containing Heterocycles. *Angew. Chem. Int. Ed.* **2018,** *130*, 583–587. (e) Luo, C. Z.; Gandeepan, P.; Wu, Y. C.; Tsai, C. H.; Cheng, C. H. Cooperative C(sp^3)–H and C(sp^2)–H Activation of 2-Ethylpyridines by Copper and Rhodium: A Route toward Quinolizinium Salts. *ACS Catal.* **2015**, *5*, 4837–4841. (f) Wu, J. Q.; Yang, Z.; Zhang, S. S.; Jiang, C. Y.; Li, Q.; Huang, Z. S.; Wang, H. From Indoles to Carbazoles: Tandem Cp*Rh(III)-Catalyzed C–H Activation/Brønsted Acid-Catalyzed Cyclization Reactions. *ACS Catal.* **2015**, *5*, 6453–6457.

(6) (a) Liu, Z.; Derosa, J.; Engle, K. M. Palladium(II)-Catalyzed Regioselective *syn*-Hydroarylation of Disubstituted Alkynes Using a Removable Directing Group. *J. Am. Chem. Soc.* **2016**, *138*, 13076–13081. (b) Zhang, J.; Shrestha, R.; Hartwig, J. F.; Zhao, P. A Decarboxylative Approach for Regioselective Hydroarylation of Alkynes. *Nat. Chem.* **2016**, *8*,

1144–1151. (c) Lou, S.-J.; Chen, Q.; Wang, Y.-F.; Xu, D.-Q.; Du, X.-H.; He, J.-Q.; Mao, Y.-J.; Xu, Z.-Y. Selective C–H Bond Fluorination of Phenols with a Removable Directing Group: Late-Stage Fluorination of 2-Phenoxyl Nicotinate Derivatives. *ACS Catal.* **2015**, *5*, 2846–2849. (d) Zhang, Y. F.; Zhao, H. W.; Wang, H.; Wei, J. B.; Shi, Z. J. Readily Removable Directing Group Assisted Chemo- and Regioselective C(sp^3)–H Activation by Palladium Catalysis. *Angew. Chem. Int. Ed.* **2015**, *54*, 13686–13690. (e) Zhang, F.; Spring, D. R. Arene C–H Functionalisation Using a Removable/Modifiable or a Traceless Directing Group Strategy. *Chem. Soc. Rev.* **2014**, *43*, 6906–6919.

(7) (a) Wang, D. H.; Wasa, M.; Giri, R.; Yu, J. Q. Pd(II)-Catalyzed Cross-Coupling of sp^3 C−H Bonds with sp^2 and sp^3 Boronic Acids Using Air as the Oxidant. *J. Am. Chem. Soc.* **2008**, *130*, 7190–7191. (b) Wasa, M.; Yu, J. Q. Synthesis of *β*-, *γ*-, and *δ*-Lactams via Pd(II)-Catalyzed C−H Activation Reactions. *J. Am. Chem. Soc.* **2008**, *130*, 14058–14059.

(8) (a) Fisher, L. E.; Caroon, J. M.; Jahangir, J.; Stabler, S. R.; Lundberg, S.; Muchowski, J. M. *O*-Methylarenehydroxamates as *ortho*-Lithiation Directing Groups. Titanium(III)-Mediated Conversion of *O*-methyl Hydroxamates to Primary Amides. *J. Org. Chem.* **1993**, *58*, 3643–3647. (b) Trend, R. M.; Ramtohul, Y. K.; Ferreira, E. M.; Stoltz, B. M. Palladium-Catalyzed Oxidative Wacker Cyclizations in Nonpolar Organic Solvents with Molecular Oxygen: A Stepping Stone to Asymmetric Aerobic Cyclizations. *Angew. Chem. Int. Ed.* **2003**, *115*, 2998–3001. (c) Wang, G. W.; Yuan, T. T. Palladium-Catalyzed Alkoxylation of *N*-Methoxybenzamides via Direct sp^2 C−H Bond Activation. *J. Org. Chem.* **2009**, *75*, 476–479.

(9) (a) Jia, Z. J.; Merten, C.; Gontla, R.; Daniliuc, C. G.; Antonchick, A. P.; Waldmann, H. General Enantioselective C−H Activation with Efficiently Tunable Cyclopentadienyl Ligands.

Angew. Chem. Int. Ed. **2017**, *56*, 2429–2434. (b) Wu, S.; Huang, X.; Wu, W.; Li, P.; Fu, C.; Ma, S. A C–H bond Activation-Based Catalytic Approach to Tetrasubstituted Chiral Allenes. *Nat. Commun.* **2015**, *6*, 7946–7954; (c) Ye, B.; Cramer, N. A Tunable Class of Chiral Cp Ligands for Enantioselective Rhodium (III)-Catalyzed C–H Allylations of Benzamides. *J. Am. Chem. Soc.* **2013**, *135*, 636–639. (d) Zeng, R.; Fu, C.; Ma, S. Highly Selective Mild Stepwise Allylation of *N*-Methoxybenzamides with Allenes. *J. Am. Chem. Soc.* **2012**, *134*, 9597–9600.

(10) (a) Li, T.; Zhou, C.; Yan, X.; Wang, J. Solvent-Dependent Asymmetric Synthesis of Alkynyl and Monofluoroalkenyl Isoindolinones by $CpRh^{III}$-Catalyzed C−H Activation. *Angew. Chem. Int. Ed.* **2018**, *57*, 4048–4052. (b) Huang, J. R.; Bolm, C. Microwave-Assisted Synthesis of Heterocycles by Rhodium(III)−Catalyzed Annulation of *N*-Methoxyamides with α-Chloroaldehydes. *Angew. Chem. Int. Ed.* **2017**, *56*, 15921–15925. (c) Tereniak, S. J.; Stahl, S. S. Mechanistic Basis for Efficient, Site-Selective, Aerobic Catalytic Turnover in Pd-Catalyzed C−H Imidoylation of Heterocycle-Containing Molecules. *J. Am. Chem. Soc.* **2017**, *139*, 14533–14541. (d) Wang, C.-Q.; Ye, L.; Feng, C.; Loh, T.-P. C−F Bond Cleavage Enabled Redox-Neutral [4+1] Annulation via C–H Bond Activation. *J. Am. Chem. Soc.* **2017**, *139*, 1762–1765. (e) Wu, X.; Wang, B.; Zhou, S.; Zhou, Y.; Liu, H. Ruthenium-Catalyzed Redox-Neutral [4+1] Annulation of Benzamides and Propargyl Alcohols via C–H Bond Activation. *ACS Catal.* **2017**, *7*, 2494–2499. (f) Gollapelli, K. K.; Kallepu, S.; Govindappa, N.; Nanubolu, J. B.; Chegondi, R. Carbonyl-Assisted Reverse Regioselective Cascade Annulation of 2-Acetylenic Ketones Triggered by Ru-Catalyzed C–H Activation. *Chem. Sci.* **2016**, *7*, 4748–4753.

(11) (a) Dai, H.; Yu, C.; Wang, Z.; Yan, H.; Lu, C. Solvent-Controlled, Tunable *β*-OAc and *β*-H Elimination in Rh(III)-Catalyzed Allyl Acetate and Aryl Amide Coupling *via* C–H Activation. *Org. Lett.* **2016**, *18*, 3410–3413. (b) Nakanowatari, S.; Ackermann, L. Ruthenium(II)-Catalyzed

C−H Functionalizations with Allenes: Versatile Allenylations and Allylations. *Chem. Eur. J.* **2015**, *21*, 16246–16251. (c) Zeng, R.; Wu, S.; Fu, C.; Ma, S. Room-Temperature Synthesis of Trisubstituted Allenylsilanes via Regioselective C–H Functionalization. *J. Am. Chem. Soc.* **2013**, *135*, 18284–18287. (d) Zhang, N.; Yu, Q.; Chen, R.; Huang, J.; Xia, Y.; Zhao, K. Synthesis of Biaryl Imino/Keto Carboxylic Acids via Aryl Amide Directed C–H Activation Reaction. *Chem. Commun.* **2013**, *49*, 9464–9466. (e) Rakshit, S.; Grohmann, C.; Besset, T.; Glorius, F. Rh(III)-Catalyzed Directed C−H Olefination Using an Oxidizing Directing Group: Mild, Efficient, and Versatile. *J. Am. Chem. Soc.* **2011**, *133*, 2350–2353.

(12) (a) Satake, S.; Kurihara, T.; Nishikawa, K.; Mochizuki, T.; Hatano, M.; Ishihara, K.; Yoshino, T.; Matsunaga, S. Pentamethylcyclopentadienyl Rhodium(III)-Chiral Disulfonate Hybrid Catalysis for Enantioselective C−H Bond Functionalization. *Nat. Catal.* **2018**, *1*, 585−591. (b) Hande, A. E.; Ramesh, V. B.; Prabhu, K. R. Rh (iii)-Catalyzed *ortho*-C(sp^2)–H Amidation of Ketones and Aldehydes Under Synergistic Ligand-Accelerated Catalysis. *Chem. Commun.* **2018**, *54*, 12113−12116. (c) Ma, Q.; Yu, X.; Lai, R.; Lv, S.; Dai, W.; Zhang, C.; Wang, X.; Wang, Q.; Wu, Y. [Cp* RhIII]/Ionic Liquid as a Highly Efficient and Recyclable Catalytic Medium for C−H Amidation. *ChemSusChem* **2018**, *11*, 3672−3678. (d) Wu, Y.; Chen, Z.; Yang, Y.; Zhu, W.; Zhou, B. Rh(iii)-Catalyzed Redox-Neutral Unsymmetrical C–H Alkylation and Amidation Reactions of *N*-phenoxyacetamides. *J. Am. Chem. Soc.* **2017**, *140*, 42−45. (e) Zheng, J.; Wang, S. B.; Zheng, C.; You, S. L. Asymmetric Synthesis of Spiropyrazolones by Rhodium-Catalyzed C(sp^2)−H Functionalization/Annulation Reactions. *Angew. Chem., Int. Ed.* **2017**, *56*, 4540−4544. (f) Park, Y.; Heo, J.; Baik, M.-H.; Chang, S. Why is the Ir(III)-Mediated Amido Transfer Much Faster Than the Rh(III)-Mediated Reaction? A Combined Experimental and Computational Study. *J. Am. Chem. Soc.* **2016**, *138*, 14020−14029. (g) Mei, R.; Loup, J.;

Ackermann, L. Oxazolinyl-Assisted C–H Amidation by Cobalt(III) Catalysis. *ACS Catal.* **2016**, *6*, 793−797. (h) Wang, H.; Lorion, M. M.; Ackermann, L. Overcoming the Limitations of C−H Activation with Strongly Coordinating *N*-Heterocycles by Cobalt Catalysis. *Angew. Chem., Int. Ed.* **2016**, *55*, 10386−10390. (i) Neufeldt, S. R.; Jiménez-Osés, G.; Huckins, J. R.; Thiel, O. R.; Houk, K. Pyridine N-oxide vs Pyridine Substrates for Rh (III)-Catalyzed Oxidative C–H Bond Functionalization. *J. Am. Chem. Soc.* **2015**, *137*, 9843−9854. (j) Park, Y.; Park, K. T.; Kim, J. G.; Chang, S. Mechanistic Studies on the Rh(III)-Mediated Amido Transfer Process Leading to Robust C–H Amination with a New Type of Amidating Reagent. *J. Am. Chem. Soc.* **2015**, *137*, 4534−4542.

(13) (a) Zhou, P.; Hu, B.; Yang, J.; Li, L.; Rao, K.; Zhu, D.; Yu, F., Two Complementary Cyclization Reactions for the Chemoselective Synthesis of Spirooxindoles. *Eur. J. Org. Chem.* **2017**, *2017*, 7256–7265. (b) Xu, H.; Zhou, B.; Zhou, P.; Zhou, J.; Shen, Y.; Yu, F.-C.; Lu, L.-L., Insights Into the Unexpected Chemoselectivity in Brønsted Acid Catalyzed Cyclization of Isatins with Enaminones: Convenient Synthesis of Pyrrolo [3, 4-c] Quinolin-1-ones and Spirooxindoles. *Chem. Commun.* **2016**, *52*, 8002–8005. (c) Parida, K. N.; Moorthy, J. N., Synthesis of *o*-Carboxyarylacrylic Acids by Room Temperature Oxidative Cleavage of Hydroxynaphthalenes and Higher Aromatics with Oxone. *J. Org. Chem.* **2015**, *80*, 8354–8360.

(14) (a) Zhao, Y.; Truhlar, D. G. The M06 Suite of Density Functionals for Main Group Thermochemistry, Thermochemical Kinetics, Noncovalent Interactions, Excited States, and Transition Elements: Two New Functionals and Systematic Testing of Four M06-Class Functionals and 12 Other Functionals. *Theor. Chem. Acc.* **2008**, *120*, 215–241. (b) Zhao, Y.; Truhlar, D. G. Density Functionals with Broad Applicability in Chemistry. *Acc. Chem. Res.* **2008**, *41*, 157–167.

(15) Frisch, M. J.; Trucks, G. W.; Schlegel, H. B.; Scuseria, G. E.; Robb, M. A.; Cheeseman, J. R.; Scalmani, G.; Barone, V.; Mennucci, B.; Petersson, G. A.; Nakatsuji, H.; Caricato, M.; Li, X.; Hratchian, H. P.; Izmaylov, A. F.; Bloino, J.; Zheng, G.; Sonnenberg, J. L.; Hada, M.; Ehara, M.; Toyota, K.; Fukuda, R.; Hasegawa, J.; Ishida, M.; Nakajima, T.; Honda, Y.; Kitao, O.; Nakai, H.; Vreven, T.; Montgomery, J. A., Jr.; Peralta, J. E.; Ogliaro, F.; Bearpark, M.; Heyd, J. J.; Brothers, E.; Kudin, K. N.; Staroverov, V. N.; Kobayashi, R.; Normand, J.; Raghavachari, K.; Rendell, A.; Burant, J. C.; Iyengar, S. S.; Tomasi, J.; Cossi, M.; Rega, N.; Millam, J. M.; Klene, M.; Knox, J. E.; Cross, J. B.; Bakken, V.; Adamo, C.; Jaramillo, J.; Gomperts, R.; Stratmann, R. E.; Yazyev, O.; Austin, A. J.; Cammi, R.; Pomelli, C.; Ochterski, J. W.; Martin, R. L.; Morokuma, K.; Zakrzewski, V. G.; Voth, G. A.; Salvador, P.; Dannenberg, J. J.; Dapprich, S.; Daniels, A. D.; Farkas, Ö.; Foresman, J. B.; Ortiz, J. V.; Cioslowski, J.; Fox, D. J. Gaussian 09, revision A.01; Gaussian, Inc.: Wallingford, CT, **2009**.

(16) (a) Hay, P. J.; Wadt, W. R. Ab Initio Effective Core Potentials for Molecular Calculations. Potentials for the Transition Metal Atoms Sc to Hg. *J. Chem. Phys.* **1985**, *82*, 270–283. (b) Hay, P. J.; Wadt, W. R. Ab Initio Effective Core Potentials for Molecular Calculations. Potentials for K to Au Including the Outermost Core Orbitals. *J. Chem. Phys.* **1985**, *82*, 299–310.

(17) (a) Hariharan, P. C.; Pople, J. A. The Influence of Polarization Functions on Molecular Orbital Hydrogenation Energies. *Theor. Chim. Acta.* **1973**, *28*, 213–222. (b) Hehre, W. J.; Ditchfield, R.; Pople, J. A. Self-Consistent Molecular Orbital Methods. XII. Further Extensions of Gaussian-Type Basis Sets for Use in Molecular Orbital Studies of Organic Molecules. *J. Chem. Phys.* **1972**, *56*, 2257–2261.

(18) (a) Ehlers, A. W.; Böhme, M.; Dapprich, S.; Gobbi, A.; Höllwarth, A.; Jonas, V.; Köhler, K. F.; Stegmann, R.; Veldkamp, A.; Frenking, G. A Set of f-Polarization Functions for Pseudo-Potential Basis Sets of the Transition Metals Sc-Cu, Y-Ag and La-Au. *Chem. Phys. Lett.* **1993**, *208*, 111–114. (b) Huzinaga, S. Gaussian Basis Sets for Molecular Calculations; Elsevier: Amsterdam: The Netherlands, **1984**.

(19) (a) Gonzalez, C.; Schlegel, H. B. Reaction Path Following in Mass-Weighted Internal Coordinates. *J. Phys. Chem.* **1990**, *94*, 5523–5527.

Table of Contents

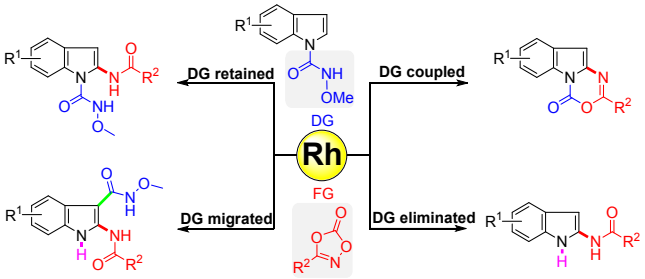

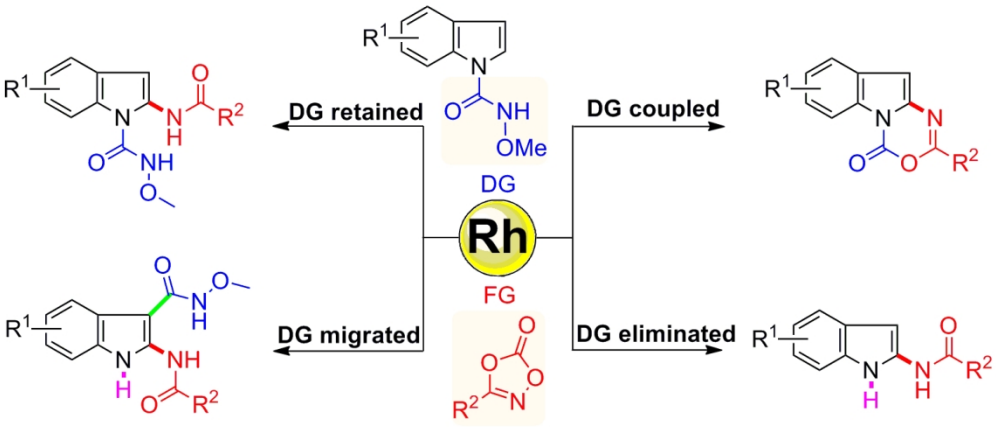

132x57mm (300 x 300 DPI)